JAST. Vol. 9, No. 1, pp 75-86

JAST
Journal of Aerospace Science and Technology

RESEARCH NOTE

Performance Modeling and Examination of Losses in the Axial -Flow Compressor

M. Eftari[1], H. Javaniyan[2] , M.R. Shahhoseini [3] , F. Ghadak[4], and M. Rad[5]

The performance prediction of axial flow compressors at different speeds and under various pressure ratio conditions are still being developed because of costly empirical experiments. One-dimensional modeling is a simple, fast and accurate method for performance prediction in any type of compressor with different geometries. In this approach, inlet flow conditions and compressor geometry are known and by considering various losses of the compressor, velocity triangles at rotor, stator inlets and outlets are determined and, then, compressor performance characteristics are predicted. Numerous models have been developed theoretically and experimentally for estimating various types of compressor losses. In the present study, the performance characteristics of the axial-flow compressor are predicted based on a one-dimensional modeling approach. Models of Lieblein, Koch-Smith, Aungier, Hawell are implemented to consider the compressor losses. To validate the model, the modeling results are compared with experimental data. This model can be used for various types of axial-flow compressors with different geometries.

***Keywords**: Axial- flow Compressor, One-dimentional Modeling , Loss Coefficient*

Nomenclature

A	Flow Cross-sectional Area (m2)
C	Actual Chord Length of Blade (m)
C_L	Blade's Lift Coefficient, Based on Mean Velocity
D_{eq}	Equivalent Diffusion Ratio
H	Height of Blades (m)
H_{TE}	Boundary-layer Shape Factor
$\dot{m}$	Mass Flow Rate of Working Fluid Through Turbo-machine (kg/s)
$\dot{m}_c$	Leakage Mass Flow Rate
W	Gas Relative Velocity with Respect to Rotor Wheel (m/s)
C_θ	Gas Tangential Velocity Component (m/s)
n	Number of Blades
N_{row}	Blade Row Number
P	Pressure (Pa)
Re_{1C}	Radius (m)
Re_{2C}	Reynolds Number at the Blade Leading Edge,
t_{max}	Maximum Blade Thickness (m)
T	Temperature (K)
U_c	Fluid Velocity of the Leakage Flow
	Pressure Loss Coefficient of a Blade
Z	Position of Maximum Camber, Measured from Blade Leading Edge

1. (Corresponding Author) M.Sc. Student, Dep't. of Mech. Eng., Young Researchers Club, South Tehran Branch, Islamic Azad University, Tehran, Iran. E-mail: Mohammad.eftari@gmail.com
2. M.Sc. Student, Dep't. of Mech. Eng., Islamic Azad University, South Tehran Branch,
3. Assistant Professor, Dep't. of Mech. Eng., Islamic Azad University, Science and Research Tehran Branch
4. Assistant Professor, Dep't. of Mech. Eng., Emam Hosein University
5. Professor, Dep't. of Mech. Eng., Sharif University of Technology

Greek

α	Angle Between C and Meridional Plane
β	Angle Between W and Meridional Plane
λ	Blade Stagger Angle
γ	Ratio of Specific Heat Capacities
γ	Blade Circulation Parameter (dimensionless)
δ^*	Boundary Layer Displacement Thickness (m)
θ	Boundary-layer Momentum Thickness (m)
κ	Peak-to-valley Surface Roughness (m)
ρ	Density (kg/m3)
ε	Blade tip Clearance
η	Isentropic Efficiency
σ_s	Blade Cascade Solidity
	Applied Loss Coefficient in Flow Equation
τ	Blades Clearance gap (m)

Subscript

a	Axial Direction
θ	Tangential Direction
EW	End Wall Losses
gap	Gap Losses
P	Profile Losses
S	Secondary Losses
TC	Tip Clearance Losses
x	Axial Component

1 Introduction

Axial-flow compressors produce a continuous flow of compressed gas, and have the benefits of high efficiency and large mass flow capacity, particularly in relation to their cross-section. They do, however, require several rows of airfoils to achieve large pressure rises, making them complex and expensive relative to other designs (e.g. centrifugal compressor).

Axial compressors are widely used in gas turbines, such as jet engines, high speed ship engines, and small scale power stations. They are also used in industrial applications[1].

Axial compressors consist of rotating and stationary components. A shaft drives a central drum which is retained by bearings and has a number of annular airfoil rows attached. These rotate between a similar number of stationary airfoil rows attached to a stationary tubular casing. The rows alternate between the rotating airfoils (rotors) and stationary airfoils (stators) with the rotors imparting energy into the fluid and the stators converting the increased rotational kinetic energy into static pressure through diffusion. A pair of rotating and stationary airfoils is called a stage. The cross-sectional area between the rotor drum and casing is reduced in the flow direction to maintain axial velocity as the fluid is compressed [2].

Performance prediction of the axial-flow compressors deals with complexities and difficulties. Although wide investigations have been done on various components of axial-flow compressors up to now, there is no model able to predict their performance characteristics accurately. Nevertheless, several theoretical and experimental models have been developed which can estimate various types of compressor losses with acceptable accuracy.

Quoting reference [3], Kesey developed a method for calculation of axial-flow compressor performance by repeating a stage model. He used a one-dimensional analysis method for performance prediction of industrial compressors.

Vincent [3] considered blade profile and end-wall losses for a multistage axial-flow compressor by repeating stage assumption and investigated its performance. He assumed that the inlet and outlet of the flow angles at each stage are the same. He also neglected the effects of height variation through the stage.

Chen et al. [4] used one-dimensional modeling for performance prediction of single-stage axial-flow compressors. They optimized the compressor efficiency by changing the absolute flow angle at the input and output of the rotor.

This study attempts to predict the performance of an axial-flow compressor by combining the most accurate models and without repetition of stage velocity triangles.

2 One-dimentional Modeling

Different methods are utilized to predict the axial-flow compressor performance. One-dimensional modeling is one of these methods.

One-dimensional modeling method is a simple and precise method which can be used for different axial compressors with different geometries. In this method, it is possible to reach the intended performance features and investigate the effect of these changes on compressor performance in order to optimize the compressor, while, in other methods, by changing the geometrical parameters, the model should be reconstructed and reperformed, which is so difficult according to the

above-mentioned explanation.

In one-dimensional modeling methods, the middle radius for one stage is considered to be constant, while the blade linear speed increases by radius enhancing. The triangle form of speeds will be changed from the hub to the tip of the blade. Here, we discuss the conditions of an average or reference radius. In fact, an average image of whatever happens during a stage on the whole mass flow will be presented by this procedure.

In one-dimensional modeling method, for simplification of the governed equations and the possibility of more quick access to performance features, the simplification hypotheses will be done as follows:

1. Input gas is considered as a perfect gas,
2. The flow will be permanent,
3. The influences of heat transfer will be ignored,
4. The atmospheric conditions will be assigned as the performance conditions,
5. The flow is one-dimentional and changes of different parameters of the flow on radial and angular directions will be disregarded and the amounts on median radius will be determined as a median amount in blade total pathway, and
6. Since the changes of the air viscosity with temperature are high, these changes will be regarded in modeling.

3 Modeling Method

The complexity of relations in compressible fluid causes the dimensional analysis of fluids to receive a special attention. This analysis creates an appropriate physical view for the prediction of fluid behavior. With the aid of the relations of dimensional analysis, we can specify four important parameters and define the other parameters according to them [5].

$$\frac{P_{03}}{P_{02}}, \eta, \frac{\Delta T_0}{T_{01}} = f\left\{\frac{\dot{m}\sqrt{RT_{01}}}{D^2 P_{01}}, \frac{ND}{\sqrt{RT_{01}}}, \mathrm{Re}, \gamma\right\} \qquad (1)$$

Hence, it is possible to determine the pressure ratio, efficiency, and decrease of relative energy according to the quantities without dimension, corresponding to mass rate, race, Reynolds number and special heat ratio. The "R" and "γ" parameters in the fluid can be considered constant and disregarded from calculations. Investigations have shown that the Reynolds number is a great parameter on turbo-machines and its changes don't have a very significant effect on other parameters [6]. The geometry is also considered constant. Hence, "D" is also deleted from the relations. Therefore, equation (1) can be restated as follows:

$$\frac{P_{03}}{P_{02}}, \eta, \frac{\Delta T_0}{T_{01}} = f\left\{\frac{\dot{m}\sqrt{T_{01}}}{P_{01}}, \frac{N}{\sqrt{T_{01}}}\right\}. \qquad (2)$$

According to equation (2), we can conclude that by the flow rate, race, and input conditions, and by using of thermodynamic relations, related equations, and geometrical dimentions, the other quantities will be calculated.

In this regard, in a step-by-step analysis, the calculations of each section will be done separately and the results of each section will be considered as the input to the next section.

In one-dimentional method, aerodynamic and thermodynamic features are considered as an average on the middle flow line. The base equations for one-dimentional isentropic flow along the channel with variable cross section include the governing equations on flow and governing relation on the perfect gas.

By Mach number relation and the above base equations, the flow equation will be extracted by considering the losses, as follows[7]:

$$\frac{\dot{m}\sqrt{\frac{RT_0}{\gamma}}}{A P_0} = \sigma \cos(\alpha) M \left(1+\frac{\gamma-1}{2}M^2\right)^{\frac{\gamma+1}{2(1-\gamma)}}. \qquad (3)$$

In this equation, "σ" is the symbol of loss coefficients and "α" is the outflow angle from the blade cascade. On the left side of the equation, "T0" and "P0" are the stagnation temperature and pressure in the input of the blade and "A" is the blade outflow area. On the right side of the equation, "M", the output Mach number, will be calculated through trial and error.

4 The Description of Solution Algorithm and Calculation of Relative and Absolute Parameters of Flow on the Axial Compressor Blade Cascade

On mathematical model, each stage is divided into two blade cascades, and the modeling of each section will be done separately.

To do the modeling calculations, in addition to the compressor geometry, the amount of rotational speed of rotor blades, the stagnation conditions of input flow to the compressor and the flow direction are assumed to be definite. By the considered amount of input Mach number, calculation will be started and, then, the mass flow rate will be calculated by continuity equation. According to the input Mach number to the blade cascade, the amount of static temperature and pressure is obtained by the following relations:

$$\frac{T_0}{T_1} = \left[1+\frac{\gamma-1}{2}M^2\right]. \qquad (4)$$

According to the governed relation on isentropic process of the perfect gas, the relation of total to static pressure ratio will be as follows:

$$\frac{P_{01}}{P_1}=\left(\frac{T_{01}}{T_1}\right)^{\frac{\gamma}{\gamma-1}}=\left[1+\frac{\gamma-1}{2}M^2\right]^{\frac{\gamma}{\gamma-1}}. \quad (5)$$

After the calculation of the input static amounts, the axial speed, the angle and relative speed of the input flow to the blade will be extracted via the speed triangle and continuity relation:

$$C_{a1}=\frac{mRT_1}{P_1A_1}\ , \quad (6)$$

$$\beta_1=\tan^{-1}\left(\frac{U}{C_{a1}}-\tan(\alpha_1)\right), \quad (7)$$

$$W_1=\frac{C_{a1}}{\cos(\beta_1)}. \quad (8)$$

The stagnation temperature relative to the rotor blade can be calculated by this relation:

$$T_{01\ rel}=T_{01}-\frac{C_1^2\left(1-\frac{\cos^2(\alpha_1)}{\cos^2(\beta_1)}\right)}{2C_p}. \quad (9)$$

By determining the relative stagnation temperature, the relative stagnation pressure will be obtained by this equation:

$$P_{01\ rel}=P_{01}\left(1-\frac{T_{01}-T_{01\ rel}}{T_{01}}\right)^{\frac{\gamma}{\gamma-1}}. \quad (10)$$

By the definition of relative parameters of input flow to rotor blade and by the flow equation, the output Mach number on blade cascade is obtained by trial and error method, and the calculation will be repeated until the convergence of output Mach number. Thus, at first the output angle and Mach number of flow will be estimated. Then, by the considered amounts for flow angle and Mach number, and by the intended loss models, the amounts of different losses coefficients and total loss coefficient will be calculated.

After this stage, the only unknown parameter in the flow equation will be Mach number. After the calculation of Mach number, in order to reach the intended accuracy (0/001) of the calculated amount, it will be necessary to continue the trial and error process.

The amount of output stagnation pressure of blade cascade is obtained by this equation as:

$$P_{01\ rel}=\sigma P_{01rel} \quad (11)$$

On the rotor blades cascade, it is assumed that there are not any heat exchanges with the surroundings. Hence, the gas relative stagnation temperature will remain fixed.

By determining the relative stagnation temperature and pressure, the amount of static temperature and pressure, according to the restated relations (4) and (5), on the rotor output section will be calculated. Then, the relative speed of the flow in this section will be obtained by the following relation:

$$W_2=2C_p\sqrt{(T_{02rel}-T_2)}. \quad (12)$$

By determining the speed and flow angle on the outlet part of rotor blades, the absolute stagnation temperature and pressure will be calculated by these relations:

$$T_{02}=T_{02rel}-\frac{W_2^2\left(1-\frac{\cos^2(\beta_2)}{\cos^2(\alpha_2)}\right)}{2C_p}, \quad (13)$$

$$P_{02}=P_{02rel}\left(1-\frac{T_{02rel}-T_{02}}{T_{02rel}}\right)^{\frac{\gamma}{\gamma-1}}. \quad (14)$$

By specifying different flow parameters for the input to the stator blade and by the use of a similar method, according to what was explained about the rotor blade cascade, Mach number and the other quantities in the stator output will be determined. After these steps and the calculation of all of the flow parameters on blade cascade, it is possible to calculate the total pressure ratio, isentropic efficiency, and other required parameters.

The steps discussed in this section will be repeated for the next stage of multi-stage compressors. All of the flow angles will be measured according to the axial direction.

Algorithm of the present compressor modeling is shown in Fig. 1.

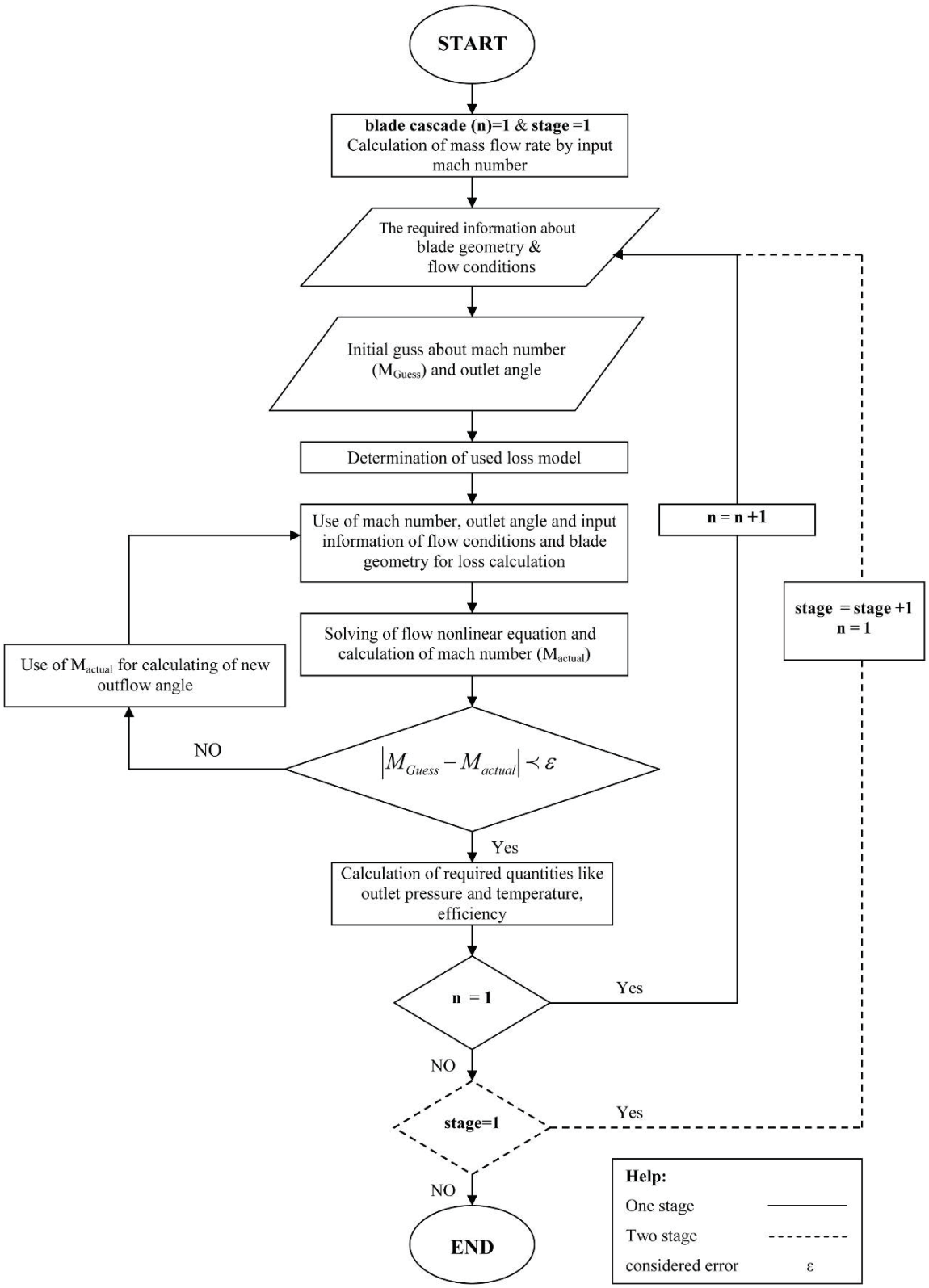

Figure 1. Algorithm of present compressor modeling.

Various sections and some geometrical dimensions of the axial-flow compressor are shown in Fig. 2. Sections 1, 2, and 3 denote the rotor inlet, rotor outlet, and stator outlet, respectively.

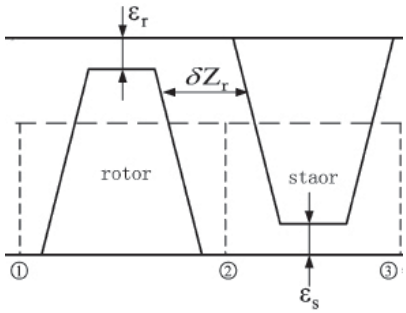

Figure 2. Schematic view of axial flow compressor sections

5 Compressor Geometry

In the present study, the performance of a two-stage axial-flow compressor without an inlet guide vane is investigated.

The compressor geometry was obtained from a NASA report [8].

6 Energy Losses

In general, when the fluid is compressible, energy losses in axial compressors will depend on many different parameters such as the incidence angle, blade chord, fluid density, fluid viscosity, Mach number, and Reynolds number.

The energy losses of axial-flow compressors are presented as loss coefficients. The conventional loss coefficients are enthalpy loss coefficient, entropy loss coefficient and stagnation pressure loss coefficient.

The pressure loss coefficients are more popular than the other loss coefficients. The loss coefficients can be specified very simply by experiments of the blade cascade.

This coefficient for compressor blades is defined as follows:

$$Y_{Rotor} = \frac{P_{01,rel} - P_{02,rel}}{P_{01,rel} - P_1}, \qquad \text{Rotor (15)}$$

$$Y_{Stator} = \frac{P_{02} - P_{03}}{P_{02} - P_2}. \qquad \text{Stator (16)}$$

Eventually, the applied loss coefficient in flow equation is:

$$\sigma = 1 - Y\left[1 - \left(1 + \frac{\gamma - 1}{2} M^2\right)^{-\gamma/(\gamma-1)}\right] \qquad (17)$$

In this equation, “M” stands for input Mach number to blade cascade.

7 Different Losses of Axial Flow Compressor

A real compressor can be thought of as an ideal machine taking in a gas at P_{01} , h_{01} , and delivering it at P'_{02th} , h'_{02} , (Fig. 3) with added losses which make the actual delivery conditions P'_{02} , h_{02} .

8 Group 1 Losses

Group 1 losses are pressure losses resulting from fluid friction. Examples are boundary-layer friction on blade and casing walls and flow-separation losses in areas of stall and blade trailing edges.

The sum of group 1 pressure losses is designated as $\sum \Delta P_{0\,g1}$ in Fig. 3.

These pressure losses reduce the outlet pressure from the theoretical P'_{02th} to P'_{02}, which is identical to P_{02} .

9 Group 2 Losses

Group 2 losses take shaft power and degrade it to an enthalpy increase in the gas discharge condition. For instance, the “windage” gas friction on compressor disks usually appears in the discharge gas state either by heat transfer through the annulus (hub) wall or, more likely, by a mass exchange of the main flow with the gas partly trapped in the cavity around the disks. In either case, the result of all such degradations of shaft power is an increase in discharge enthalpy from h′02 to h02. The sum of group 2 losses is designated as $\sum \Delta h_{0\,g2}$ in Fig. 3.

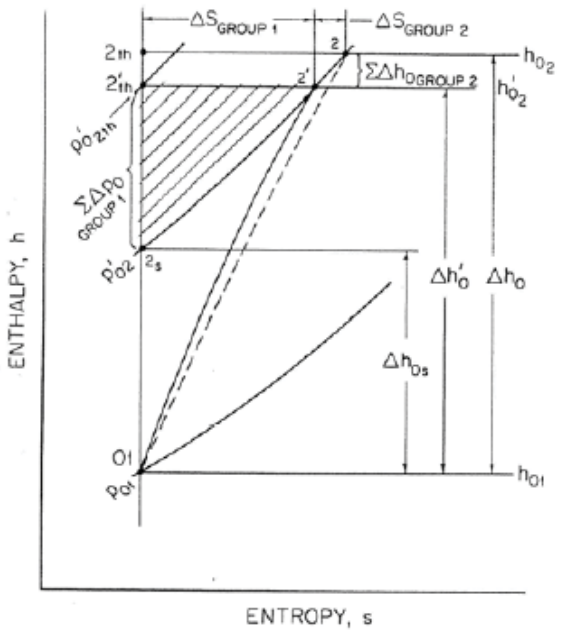

Figure 3. Loss representation in h-s diagram

10 Group 3 Losses

Group 3 losses are losses of shaft power through friction whose energy is dissipated away from the working fluid.

Examples are the friction losses in external bearings and seals. The power losses appear as increases in compressor power requirements.

11 Isentropic Efficiency

By definition, we have:

$$\eta_{is} \equiv \frac{\Delta h_{0is}}{\Delta h_0} = \frac{\Delta h_{0is}}{\Delta h_0' + \sum \Delta h_{0g2}}$$

$$= \frac{\bar{C}p_{1-2is}\left(T_{02is} - T_{01}\right)}{\bar{C}p_{1-2'}\left(T_{02}' - T_{01}\right) + \bar{C}p_{2'-2}\sum \Delta T_{0g2}}, \quad (18)$$

where

$$r \equiv p_{02}/p_{01},$$

$$\eta_{is} = \frac{r^{R/\bar{C}p_{1-2s}} - 1}{\left(\bar{C}p_{1-2'}/\bar{C}p_{1-2s}\right)\left\{\left[r + \left(\sum \Delta p_{0g1}\right)/p_{01}\right]^{R/\bar{C}p_{1-2}} - 1\right\} + \sum \Delta h_{0g2}/\bar{C}p_{1-2s}T_{01}}. \quad (19)$$

In a preliminary design, the specific-heat ratio ($Cp_{1\text{-}2'}/Cp_{1\text{-}2s}$) is often taken to be unity.

The final state after compression is P_{02} , h_{02} . This point can be considered to be arrived at directly by the process line shown dashed in Fig. 3. or two processes could be conceptually involved: points 01 to 2′, with just group 1 (pressure) losses: and 2′ to 2, with just shaft-power (energy) losses (group 2). Or we could think of an ideal (isentropic) process over the actual enthalpy rise from 01 to 2_{th} . followed by a pure increase of entropy from 2_{th} to 2, a throttling process, being the sum of the entropy increases due to group 1 and 2 losses.

12 Loss Coefficient in Compressor Blades

In this section, Reynolds and Mach numbers are based on the relative gas flow velocities. The total pressure loss coefficient in the compressor is given as:

$$Y = Y_P + Y_S + Y_{EW} + Y_{TC}. \quad (20)$$

13 Blade-profile Loss

Lieblein [9] expressed the blade-profile pressure loss coefficient as:

$$Y_p = 2\left(\frac{\theta_2}{C}\right) \times \frac{\sigma_s}{\cos\beta_2} \times \left(\frac{\cos\beta_1}{\cos\beta_2}\right)^2 \times \left(\frac{2H_{TE}}{3H_{TE} - 1}\right) \times \left[1 - \left(\frac{\theta_2}{C}\right)\frac{\sigma H_{TE}}{\cos\beta_2}\right]^{-3}. \quad (21)$$

The boundary-layer momentum thickness at the blade outlet, , is given [10] as:

$$\frac{\theta_2}{C} = \left(\frac{\theta_2^0}{C}\right) \times \zeta_M \times \zeta_H \times \zeta_{\mathrm{Re}}. \quad (22)$$

The boundary layer trailing-edge shape factor, H_{TE}, the ratio of the boundary layer displacement thickness to the momentum thickness, θ_2 , is expressed as:

$$H_{TE} = H_{TE}^{0} \times \xi_M \times \xi_H \times \xi_{\mathrm{Re}}. \quad (23)$$

The values of and are for inlet Mach numbers, $M_{a1} < 0.05$, no contraction in the height of the flow annulus, H , an inlet Reynolds number, $\mathrm{Re}_{1c} = 10^6$ and hydraulically smooth blades. Based on the experimental data of Koch and Smith [10] under these conditions, the boundary-layer momentum thickness at the blade outlet is correlated accurately as:

$$\frac{\theta_2}{C} = 2.644\times10^{-3} \times D_{eq} - 1.519\times10^{-4} + \frac{6.713\times10^{-3}}{2.60 - D_{eq}}. \quad (24)$$

The shape factor for the boundary layer trailing-edge is correlated as:

$$H_{TE}^{0} = \frac{\delta_{TE}^{*}}{\theta_2^{0}} = \left(0.91 + 0.35\times D_{eq}\right) \times\left\{1 + 0.48\times\left(D_{eq} - 1\right)^4 + 0.21\times\left(D_{eq} - 1\right)^6\right\}. \quad (25)$$

The value of $H_{TE}^{\circ} = 2.7209$ is used when $D_{eq} > 2.0$. For conditions other than nominal, Koch and Smith developed charts for determining the correction factors ζ_m , ζ_H , ζ_{Re} in Eq. (22) and ξ_m , ξ_H , ξ_{Re} in Eq. 23. The correction factor for inlet Mach number is correlated as:

$$\zeta_M = 1.0 + \left(0.11757 - 0.16983\times D_{eq}\right)\times M_1^{n}, \quad (26)$$

$$n = 2.853 + D_{eq}\left(-0.97747 + 0.19477\times D_{eq}\right). \quad (27)$$

The correction factor for the flow area contraction is given by:

$$\zeta_H = 0.53\frac{H_1}{H_2} + 0.47. \quad (28)$$

The chart presented by Koch and Smith for the Reynolds correction factor is well approximated using the approach proposed by Aungier [11]. He introduced the critical blade chord Reynolds number, $\mathrm{Re}_{cr} = 100\times\frac{c}{\kappa}$, above which the effect of roughness become significant. When $\mathrm{Re}_{1c} < \mathrm{Re}_{cr}$, the Reynolds correction factor is expressed as:

$$\zeta_{\mathrm{Re}} = \begin{cases} \left(\dfrac{10^6}{\mathrm{Re}_{1C}}\right)^{0.166}, & \text{for } \mathrm{Re}_{1C} \geq 2\times10^5, \\ 1.30626\times\left(\dfrac{2\times10^5}{\mathrm{Re}_{1C}}\right)^{0.5}, & \text{for } \mathrm{Re}_{1C} < 2\times10^5. \end{cases} \quad (29)$$

When $\mathrm{Re}_{1c} > \mathrm{Re}_{cr}$, the friction losses are controlled by the surface roughness and the Reynolds correction factor may be expressed as:

$$\zeta_{\mathrm{Re}} = \begin{cases} \left(\dfrac{10^6}{\mathrm{Re}_{cr}}\right)^{0.166}, & \text{for } \mathrm{Re}_{cr} \geq 2\times10^5, \\ 1.30626\times\left(\dfrac{2\times10^5}{\mathrm{Re}_{cr}}\right)^{0.5}, & \text{for } \mathrm{Re}_{cr} < 2\times10^5. \end{cases} \quad (30)$$

Typical ratios of the blade chord to surface roughness are: $c/\kappa = 10{,}000$ to $20{,}000$. When $\mathrm{Re}_{1c} > 10^6$ and $c/\kappa = 10^4$, $\mathrm{Re} = 10^6$ and $\zeta_{\mathrm{Re}} = 1$. The correction factor for the inlet Mach number is accurately fitted by:

$$\xi_M = 1.0 + \left[1.0725 + D_{eq}\times\left(-0.8671 + 0.18043\times D_{eq}\right)\right]\times M_1^{1.8}. \quad (31)$$

The correction factor for the flow area contraction is calculated as:

$$\xi_H = 1.0 + \left(\frac{H_1}{H_2} - 1.0\right) \times \left(0.0026 \times D_{eq}^8 - 0.024\right). \quad (32)$$

The correction factor for the inlet Reynolds number is given by:

$$\xi_{\mathrm{Re}} = \begin{cases} \left(\dfrac{10^6}{\mathrm{Re}_{1C}}\right)^{0.06}, & When \quad \mathrm{Re}_{1C} < \mathrm{Re}_{cr}, \\ \left(\dfrac{10^6}{\mathrm{Re}_{cr}}\right)^{0.06}, & When \quad \mathrm{Re}_{1C} \geq \mathrm{Re}_{cr}. \end{cases} \quad (33)$$

The equivalent diffusion ratio, D_{eq} is given by [10]:

$$D_{eq} = \frac{W_1}{W_2} \times \left[1 + K_3 \frac{t_{\max}}{C} + K_4 \Gamma^*\right] \times \sqrt{\left(\sin\beta_1 - K_1 \sigma_s \Gamma^*\right)^2 + \left(\frac{\cos\beta_1}{A^*_{throat} \times \rho_{throat}/\rho_1}\right)^2}. \quad (34)$$

In Eq. (34), the contraction ratio is given by:

$$A^*_{throat} = \left[1 - K_2 \sigma_s \left(\frac{t_{\max}}{c}\right) \Big/ \cos\overline{\beta}\right]\left(1 - \frac{A_{throat}}{A_1}\right), \quad (35)$$

$$\overline{\beta} = \frac{\beta_1 + \beta_2}{2}. \quad (36)$$

The throat area is assumed to occur at one-third of the axial chord, thus:

$$A_{throat} = A_1 - \frac{1}{3}\left(A_1 - A_2\right). \quad (37)$$

The gas density at the throat is calculated as:

$$\frac{\rho_{throat}}{\rho_1} = 1 - \frac{M_x^2}{1 - M_x^2}\left(1 - A^*_{throat} - K_1 \frac{\tan\beta_1}{\cos\beta_1} \sigma_s \Gamma^*\right). \quad (38)$$

The obtained constants in these equations from the experimental data of Koch and Smith are: D_{eq}, $k_2 = 0.4458$, $k_3 = 0.7688$ and $k_4 = 0.6024$. The dimensionless blade circulation parameter in Eq's. 34-38 is given by:

$$\Gamma^* = \frac{r_{1m} C_{1\theta} - r_{2m} C_{2\theta}}{\sigma_s W_1 \times \left(r_{1m} - r_{2m}\right)/2} = \left(\tan\beta_1 - \tan\beta_2\right) \times \frac{\cos\beta_1}{\sigma_s}. \quad (39)$$

9 Secondary Flow Loss

The secondary flow loss coefficient is given by the correlation proposed by Howell [12] as:

$$Y_S = 0.018 \times \sigma_s \times \frac{\cos^2\beta_1}{\cos^3\beta_m} \times C_L^2. \quad (40)$$

The theoretical compressor blade lift coefficient, C_L, is expressed as:

$$C_L = \frac{2}{\sigma_s} \times \cos\left(\beta_m\right) \times \left[\tan\left(\beta_1\right) - \tan\left(\beta_2\right)\right]. \quad (41)$$

The mean velocity vector angle is given by:

$$\tan(\beta_m) = 0.5 \times \left[\tan(\beta_1) + \tan(\beta_2)\right]. \quad (42)$$

End-Wall Boundary Layer Analysis

The flow in the end-wall regions has a substantial influence on the aerodynamic performance of axial-flow compressors. A significant portion of the losses in axial-flow compressors is directly associated with the end-wall flow.

In addition, individual stage loading limits and the compressor surge flow limit are often associated with end-wall stall.

Unfortunately, there is no available theoretical aerodynamic model capable of predicting the detailed behavior of these highly complex end-wall flows. Indeed, even modern computational fluid dynamics (CFD) viscous flow solvers are found to be incapable of resolving many of the important flow patterns that are observed in the end-wall regions of axial-flow compressors. When fundamental analysis techniques are not sufficient to treat a problem of interest, engineers commonly resort to a combination of theoretical and empirical models.

14 End Wall Loss

Based on a modified Howell's model [12], Aungier [11] developed the following expression for calculating the end wall loss coefficient, as:

$$Y_{EW} = 0.0146 \times \frac{C}{H} \times \frac{\cos^2 \beta_1}{\cos^2 \beta_2}. \quad (43)$$

15 Tip Clearance Loss

These losses are due to the existence of a gap between the end of the rotary blades and the inside walls of the compressor.

The calculation of the blade tip clearance loss is based on the same semi-empirical model by Aungier. Figure (4) shows the tip clearance geometry for a typical rotor blade.

The pressure difference on the two sides of the blade produces a leakage flow through the clearance gap, basically dissipating the pressure difference. The pressure difference across the blade must balance the blade torque. For the clearance gap, this can be expressed as:

$$\begin{aligned} \tau &= \dot{m}[r_2 c_{\theta 2} - r_1 c_{\theta 1}], \\ &= \pi \varepsilon [(r \rho c_a)_1 - (r \rho c_a)_2][r_2 c_{\theta 2} - r_1 c_{\theta 1}]. \end{aligned} \quad (44)$$

The average pressure difference across each blade in the blade row is:

$$\Delta P = \tau / (n r_1 \varepsilon \cos \lambda), \quad (45)$$

where, "n" is the number of blades in the blade row.

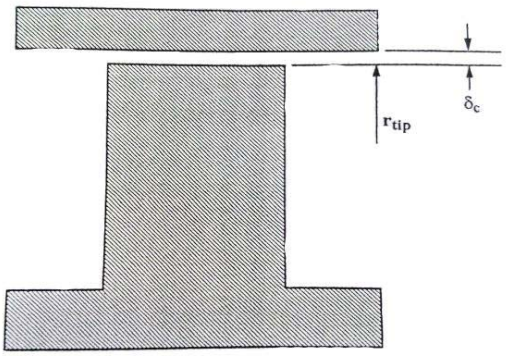

Figure 4 . Blade Tip Clearance Geometry.

The fluid velocity of the leakage flow, which is maximum in the first blade row, is estimated from ΔP, but is reduced as the blade row number, N_{row}, increases, i.e.

$$U_c = 0.816 \sqrt{2\Delta P / \overline{\rho}} \Big/ N_{row}^{0.2}. \quad (46)$$

The end wall boundary layer growth in multistage axial-flow compressors results in a substantial tangential blade force defect which is expected to reduce the tip leakage flow. The dependence on N_{row} was determined empirically from the comparison of the predicted and measured performance of several multistage axial-flow compressors. The leakage mass flow rate is given by:

$$\dot{m}_c = \overline{\rho} U_c n \varepsilon \cos \lambda. \quad (47)$$

The clearance gap total pressure loss for the entire blade row is:

$$\Delta P_{0C} = \Delta P \dot{m}_c / \dot{m}, \quad (48)$$

$$Y_P = \frac{\Delta p_{0C}}{\left[\rho_1 W_1^2/2\right]}. \quad (49)$$

11 Results and Discussion

Figure 5 shows variation of the compressor pressure ratio versus mass flow at 11230 rpm that was compared with the experimental data of a NASA report [8]. It is in a good agreement with 1.69% of the maximum difference.

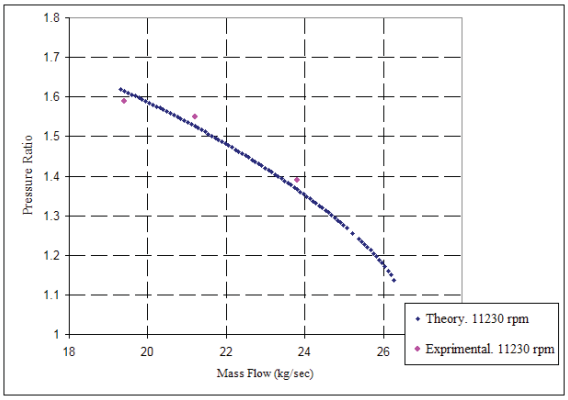

Figure 5. Pressure ratio vs mass flow at 11230 rpm.

The comparison of the achieved results of modeling with the experimental results of the NASA report [8] are presented in Table 1.

Table1. Results of present model and NASA report

Mass Flow (Kg/sec)	PR of present model	PR of NASA report	Relative error percent
19.4	1.614841563	1.59	1.56
21.2	1.525660408	1.55	1.57
23.8	1.366382607	1.39	1.69

According to the resulting curves from modeling in Fig. 6, that are related to the pressure ratio diagram on the mass flow of a two-stage compressor, it has been observed that at a fixed speed, by the increase of mass flow, the compressor pressure ratio will decrease and at higher mass flow, the loss of pressure ratio becomes greater because, in these conditions, the compressor losses will increase.

The increases of mass flow amount are infinite but lead to a definite amount. This amount is related to a state in which Mach number will reach one in a section of the blade (throat) and damping phenomenon will happen. The place of the occurrence of damping phenomenon is between the rotating blades (Rotor) of the compressor because, according to the figure, the damping area is dependent on the rotational speed of the blade and, by the change of speed, the damping mass flow rate changes too. Also, at a fixed rotational speed, by an decrease in mass flow, the pressure ratio changes and ultimately reaches its maximum value. By further decrease in mass flow rate, the inside flow of the compressor will be unstable, a phenomenon which is called surge. The mechanism of surge in an axial compressor is very complicated.

Also, at a fixed mass flow, by a decrease in compressor speed, the pressure ratio will increase, which is due to the increase of the special work of the compressor because the work of the compressor is directly related to the blade speed.

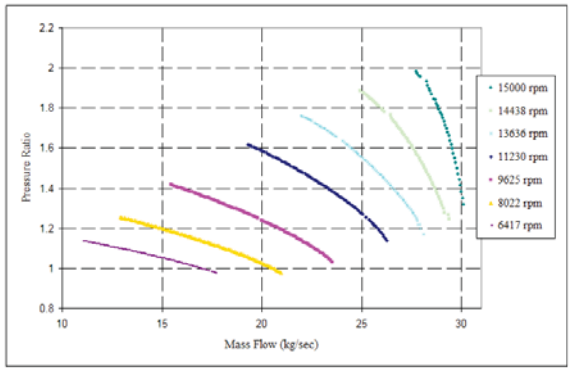

Figure 6. Pressure ratio vs mass flow at different rpm.

Variation of compressor isentropic efficiency versus mass flow at various speeds is shown in Fig. 7. As seen, the curves of efficiency versus mass flow at each speed have a maximum point and, by departing from this point, efficiency decreases because of loss grooving, which is more intensive at high mass flows.

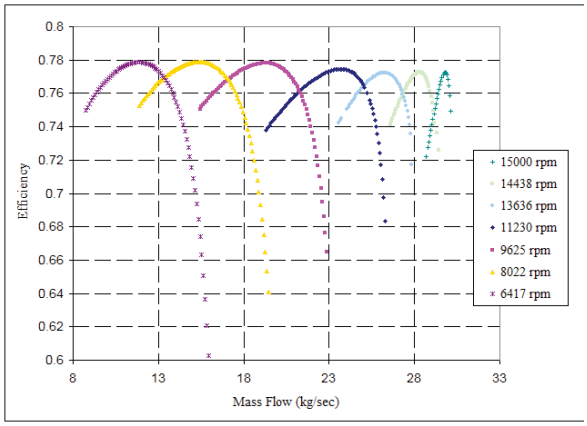

Figure 7. Compressor efficiency vs mass flow at different rpm.

Variation of compressor isentropic efficiency versus pressure ratio at various speeds is shown in Fig. 8.

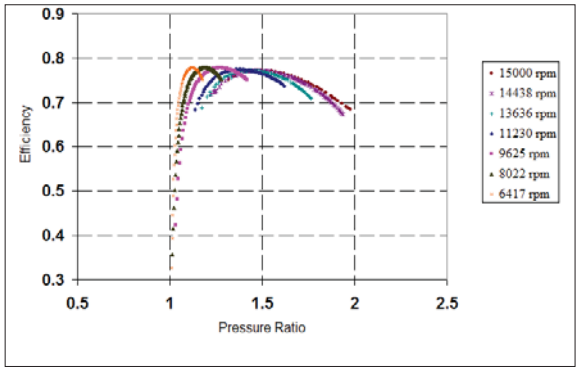

Figure 8. Compressor efficiency vs pressure ratio at different rpm.

Figure 9 shows variation of Profile loss coefficient, Secondary loss coefficient , End Wall loss coefficient, tip clearance loss coefficient and Total loss coefficient as a function of pressure ratio at 11230 rpm . It is observed that at constant speeds, compressor loss coefficients increase as pressure ratio increases.

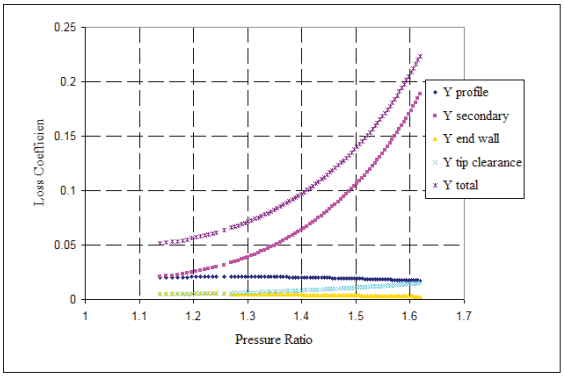

Figure 9. Loss coefficients vs pressure ratio at 11230 rpm.

16 Conclusions

In the present study, performance of a two-stage axial-flow compressor is investigated using a one-dimensional modeling approach. Previous models are used to develop a comprehensive model, which is not found in the open literature.

At 11230 rpm, the results are compared with the experimental data of NASA. The maximum error observed is about 1.69% and the results are in a good agreement with those of the NASA experiment. Given that the one-dimensional modeling approach has some advantages such as simplicity, rapidity and applicability, this error can be neglected.

17 References

1. Schobeiri.M “Turbomachinery Flow Physics and Dynamic Performance” Texas A&M University,2005. turbomachines “ McGraw-Hill Book Co ,1990

2. Cohen, H. , Rogers, C. , and Saravanamutto, .H “Gas Turbine Theory” Longman group ,1996

3. Vincent, A. “Impact of geometric variability on repeating stage compressor performance” M.Sc. Thesis, Massachusetts institute of technology, 2003.

4. Lingen Chen, Jun Luo, Fengrui Sun, and Chih Wu, “Optimized efficiency axial-flow compressor” Elsevier Applied Energy, 2005.

5. Whitfield, A. and Baianes, N. C.”A general computer solution for radial and mixed flow turbomachine performance prediction.” IMech., Vol. 18, PP.184-19 ,1976.

6. Sayers, A.T. “Hydraulic and compressible flow turbomachines “ McGraw-Hill Book Co ,1990

7. Whitfield. A., baines. N.C. “Design of radial turbomachines “ Impeial college of science, London, 1976.

8. Schmidt, J.F.”Off-Design Computer Code for Calculating the Aerodynamic Performance of Axial-Flow Fans and Compressors”, NASA Contractor Report 198362,1995

9. Lieblein, S. “Loss and Stall analysis in compressor cascades” J Basic Eng 1959;81:387-400

10. Koch, C.C., and Smith L.H. ” Loss Sources and Magnitude in Axial-Flow Compressors” journal of Engineering for Power, ,pp.411-424, 1976

11. Aungier, R.H. ”A Strategy for Aerodynamic Design and Analysis”,Asme Press ,2003

12. Howell, A.R. “Fluid dynamics of axial compressors.” No.12;1947 GreatBritian.p.441-52